ALD Precursors

Deutsche Ausgabe: DOI: 10.1002/ange.201602406
Internationale Ausgabe: DOI: 10.1002/anie.201602406

Synthesis of Calcium(II) Amidinate Precursors for Atomic Layer Deposition through a Redox Reaction between Calcium and Amidines

*Sang Bok Kim, Chuanxi Yang, Tamara Powers, Luke M. Davis, Xiabing Lou, and Roy G. Gordon**

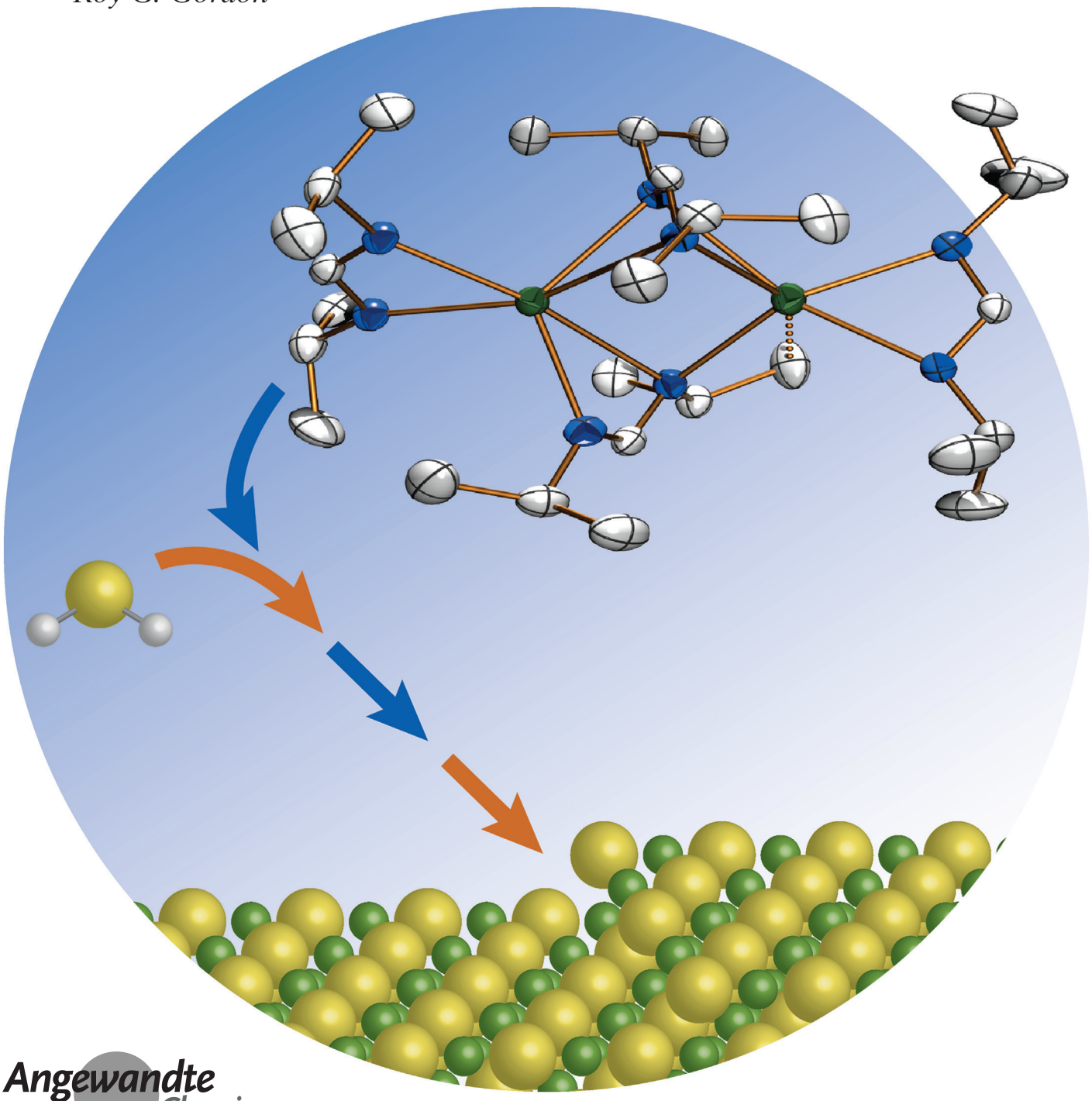

Abstract: *We have prepared two new Ca^{II} amidinates, which comprise a new class of ALD precursors. The syntheses proceed by a direct reaction between Ca metal and the amidine ligands in the presence of ammonia. Bis(N,N′-diisopropylformamidinato)calcium(II) (**1**) and bis(N,N′-diisopropylacetamidinato)calcium(II) (**2**) adopt dimeric structures in solution and in the solid state. X-ray crystallography revealed asymmetry in one of the bridging ligands to afford the structure $[(\eta^2\text{-L})Ca(\mu\text{-}\eta^2\text{:}\eta^2\text{-L})(\mu\text{-}\eta^2\text{:}\eta^1\text{-L})Ca(\eta^2\text{-L})]$. These amidinate complexes showed unprecedentedly high volatility as compared to the widely employed and commercially available Ca^{II} precursor, $[Ca_3(tmhd)_6]$. In CaS ALD with **1** and H_2S, the ALD window was approximately two times wider and lower in temperature by about 150 °C than previously reported with $[Ca_3(tmhd)_6]$ and H_2S. Complexes **1** and **2**, with their excellent volatility and thermal stability (up to at least 350 °C), are the first homoleptic Ca^{II} amidinates suitable for use as ALD precursors.*

Calcium plays an important role in a wide variety of multicomponent materials, including nonlinear optics,[1] phosphors,[1] dielectrics,[2] high-temperature superconductors,[3] colossal magnetoresistance materials,[4] planar waveguides,[5] laser windows, and fiber optics.[5] Promising potential applications of calcium oxide, owing to its wide band gap of 6.8 eV,[6] include alloys with HfO_2 for gate-capacitor dielectrics in metal-oxide-semiconductor field-effect transistors (MOSFETs),[5] and alloys with MgO as an epitaxial gate insulator in GaN-based high-electron-mobility transistors (HEMTs).[5,7] Calcium sulfide may have utility as an alloy with the strong visible-light absorber SnS; the addition of calcium to SnS to form $Sn_{1-x}Ca_xS$ stabilizes the desirable but unstable cubic (rock-salt) phase of this material.[8]

For many of these applications, especially in electronic devices, a method to deposit uniform thin films at modest temperatures is required. Atomic layer deposition (ALD), a modified form of chemical vapor deposition in which precursors are delivered in pulses, provides a route to conformal thin films of metals, metal oxides, and metal chalcogenides even on nanostructured substrates.[9] During each pulse cycle, one precursor reacts with the growth surface until the surface is saturated, and then by-products and unreacted precursor are removed by purging with inert gas.[9] This process is repeated alternately, and the self-limiting character (film growth through surface saturation) allows for accurate and reproducible control of film thickness with excellent large-area uniformity and conformality.[9] Other requirements for an ALD precursor are self-limited reactivity with the growth surface, high volatility, high thermal stability, and the formation of only stable and noncorrosive by-products.[9]

ALD affords a constant film-growth rate within a temperature window; at lower temperatures, the precursor may not react with the surface or may condense without any surface reaction, whereas at higher temperatures, the precursor may decompose. The available ALD window is critically important in the selection of precursors for multicomponent thin films,[10] whereby the temperature range is defined by the overlap of the individual component ALD windows. Therefore, a major goal of ALD precursor development is increasing the growth window, and this goal is especially urgent for calcium because Ca has mostly been alloyed with metal chalcogenides and metal oxides for functional-materials applications.

The most widely employed ALD Ca precursor,[4,11] commercially available trimeric $[Ca_3(tmhd)_6]$ (tmhd = 2,2,6,6-tetramethylheptane-3,5-dionate),[11a,c,d,12] has an ALD window of 325–400 °C for the ALD of CaS with H_2S as a coprecursor.[11a,b] One alternative precursor, $[Ca(i\text{Pr}_3\text{Cp})_2]$ ($i\text{Pr}_3\text{Cp}$ = 1,2,4-triisopropylcyclopentadienyl),[13] has a somewhat lower window in the ALD of CaO films with H_2O as a coprecursor (200–300 °C, 1–2 atom % carbon),[5,11d] but has not seen widespread adoption.

Several other types of volatile Ca^{II} complexes (fluoroalkoxides,[14] fluorinated β-diketonates,[15] β-diketiminates,[16] and aminodiboranates[17]) have been reported, but not employed in ALD reactions. To complement the currently known Ca ALD precursors, we chose to explore the amidinate ligand system. Amidinate ligands have high basicity, and amidinate complexes have been shown to react readily with proton sources, such as H_2O and H_2S, for the ALD of a variety of transition-metal and lanthanide oxides and sulfides.[18] Although several Ca^{II} amidinate complexes are known (Scheme 1), none are appropriate for ALD. All of the ligands contain bulky aryl groups, which typically afford compounds of very low volatility.

Herein, we report the synthesis of Ca^{II} alkyl amidinates with excellent thermal stability and volatility, and demonstrate the utility of one of the complexes in the ALD of CaS. Dimeric bis(*N*,*N*′-diisopropylformamidinato)calcium(II) (**1**; 57 % yield; distills at 110–115 °C, 0.2 torr) and dimeric bis(*N*,*N*′-diisopropylacetamidinato)calcium(II) (**2**; 59 % yield; sublimes at 120–125 °C, 0.1 torr) were prepared in the presence of ammonia[19] by an atom-economical redox reaction between Ca metal and the free amidines[18a,20] (Scheme 2). This direct synthesis avoids the involvement of other metals and reduces the possibility of incorporating trace metal contaminants into thin films. The mechanism probably follows that of the reaction of Ca with $HN(SiMe_3)_2$ to form $Ca[N(SiMe_3)_2]_2(THF)_2$.[19] **1** and **2** are the first nitrogen-only coordinated Ca^{II} complexes that satisfy the ALD requirements of high volatility and thermal stability. For example,

[*] Dr. S. B. Kim, C. Yang, Dr. L. M. Davis, X. Lou, Prof. Dr. R. G. Gordon
Department of Chemistry and Chemical Biology, Harvard University
12 Oxford Street, Cambridge, MA 02138 (USA)
E-mail: gordon@chemistry.harvard.edu
Dr. T. Powers
Department of Chemistry, Texas A&M University
College Station, TX 77843-3255 (USA)

Supporting information, including experimental details (syntheses, ALD procedures, and characterization), and the ORCID identification number(s) for the author(s) of this article can be found under http://dx.doi.org/10.1002/anie.201602406.

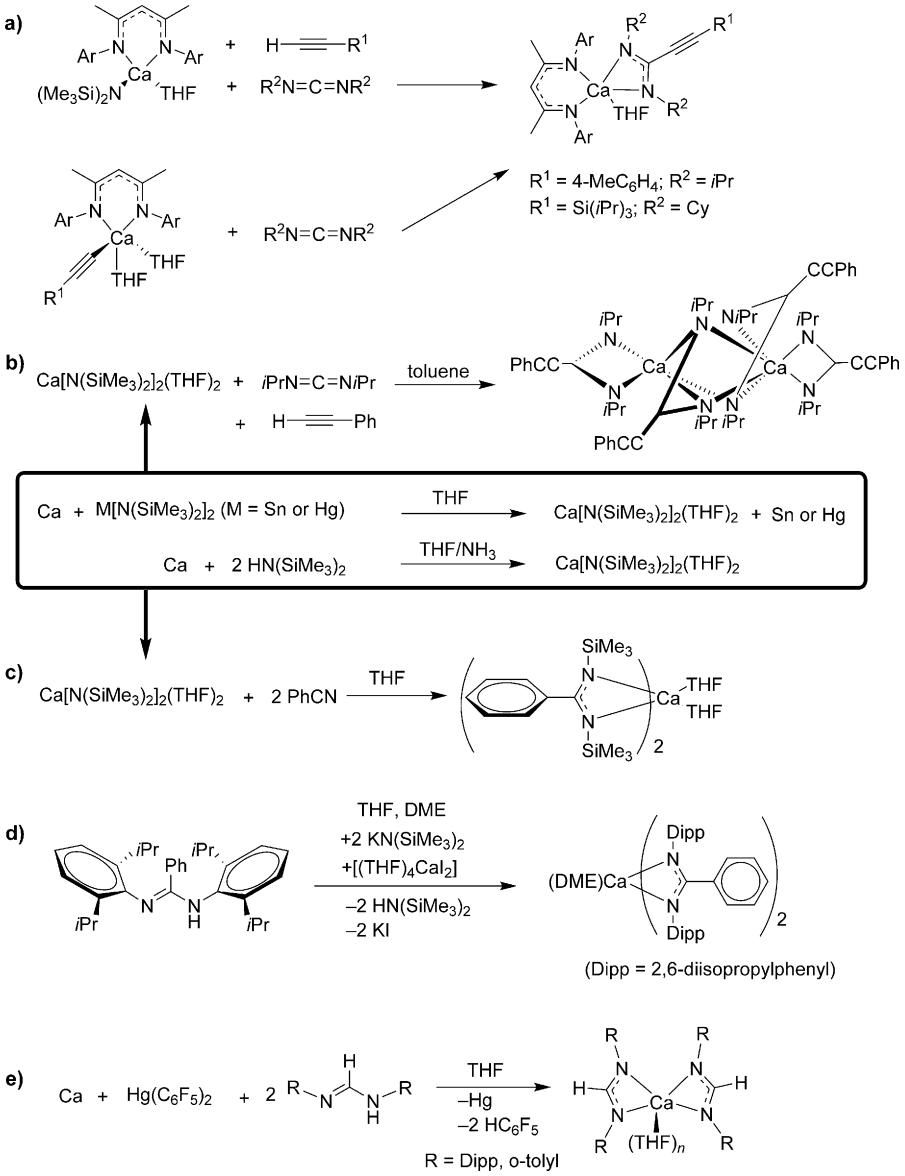

Scheme 1. Previously reported synthetic routes to Ca^{II} amidinates, prepared by a,b) protonolysis and carbodiimide insertion,[21] c) phenyl cyanide insertion,[22,23] d) salt metathesis,[24] and e) redox transmetalation.[25] Cy = cyclohexyl, Ar = Aryl, DME = 1,2-dimethoxyethane.

although homoleptic β-diketiminate Ca^{II} complexes are appreciably volatile, they decompose at about 180 °C and are therefore not suitable for ALD.[16]

Single-crystal X-ray analysis[27] (Figure 1; see also Tables S1–S3 in the Supporting Information) showed that, in the solid state, **1** is a homoleptic dimer in which each Ca center is coordinated by one terminal bidentate amidinate and two bridging amidinates. One of the bridging ligands (N(5) and N(6)) coordinates to both Ca centers in a symmetric fashion (μ-η^2:η^2). The other bridging ligand (N(7) and N(8)) coordinates in an asymmetric fashion (μ-η^2:η^1). Therefore, formally the coordination number at Ca(1) is six, whereas the coordination number at Ca(2) is only five, as found in one previously reported Ca^{II} amidinate.[21a] Interestingly, the sixth (vacant) coordination site of Ca(2) appears to be filled by an agostic interaction with C(24): The Ca···H distances of 2.80 and 2.84 Å fall at the long end of the range typically described as agostic.[26] The Ca–N bond lengths (see Table S2) are consistent with those found in other Ca^{II} amidinates. The terminal Ca–N distances of 2.323(3)–2.375(3) Å fall at the short end of the range reported for terminal amidinates, 2.306(5)–2.525(3) Å,[24] with most distances in the range 2.36–2.44 Å.[21a,24,25] The Ca(2)–N distances (2.324(3), 2.325(3) Å) are shorter than the Ca(1)–N distances (2.347(3), 2.374(3) Å), as should be expected from the lower coordination number of Ca(2). The bridging Ca–N distances (2.400(3)–2.633(3) Å) are slightly shorter than those found in the only previously reported bridging amidinate (2.445(3)–2.650(3) Å).[21a] The Ca(1)–N(8) distance of 2.407(4) Å reflects the η^1 nature of this nitrogen atom, and the Ca(2)–N(8) distance of 3.545(4) Å is nonbonding. Although extreme disorder and weak diffraction thwarted the refinement of several data sets for **2**, the connectivity of **2** does appear to be the same as found in **1**. ^{1}H and ^{13}C NMR spectroscopy clearly showed that **1** and **2** maintain dimeric structures in solution (see Figures S1 and S2 in the Supporting Information).

Thermogravimetric analysis (TGA) was used to investigate the volatility and thermal stability of **1** and **2**. Under a linear temperature ramp, quantitative, single-step weight loss was observed in the temperature range 150–275 °C for **1** and 175–290 °C for **2** (Figure 2a). Therefore, both **1** and **2** can vaporize without decomposition (i.e., **1** and **2** are thermally stable) in those temperature ranges on the time scale of the TGA experiment. With a larger sample and faster heating rate, the weight-loss window was elevated as expected, and quantitative, single-step weight loss occurred in the range of 300–400 °C (Figure 2a). The excellent thermal stability of both complexes to at least 350 °C meets an important requirement for ALD, namely, thermal stability during mass transport to the substrate surface at film-growth temperatures.

Evaporation rates for **1**, **2**, and $[Ca_3(tmhd)_6]$, obtained from isothermal TGA experiments (Figure 2b; see also Figure S5), show that the evaporation rates (i.e., volatilities) follow the order $\mathbf{1} > \mathbf{2} > [Ca_3(tmhd)_6]$. Notably, the evaporation rate of **1** was approximately 37 times higher than that of $[Ca_3(tmhd)_6]$ at 225 °C, at which temperature both compounds

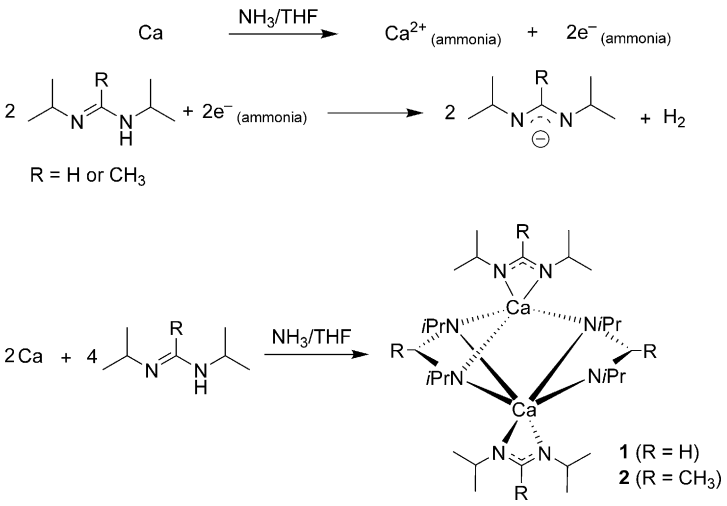

Scheme 2. Synthesis of Ca^{II} amidinates by a redox reaction between Ca metal and an amidine. a) Plausible redox reaction mechanisms for Ca and the amidine. b) Synthesis of **1** and **2**.

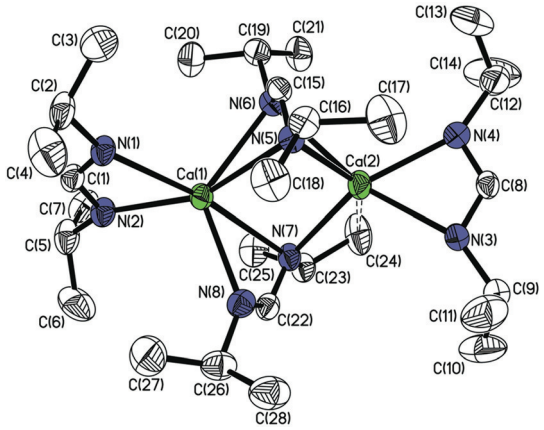

Figure 1. Solid-state structure of **1** with the thermal ellipsoids set at the 30% probability level; hydrogen atoms and the minor positions (15%) of the disordered bridging ligands are omitted for clarity. Selected distances [Å]: Ca(1)–N(1) 2.347(3), Ca(1)–N(5) 2.633(3), Ca(1)–N(7) 2.619(3), Ca(1)–N(8) 2.407(4), Ca(2)–C(24) 3.102(6).[27]

are liquid (m.p. of **1**: 110–116 °C; m.p. of $[Ca_3(tmhd)_6]$: 220–223 °C). The slopes of the logarithms of evaporation rate versus inverse temperature in Figure 2b indicate that the enthalpy of vaporization is lower for **1** and **2** than for $[Ca_3(tmhd)_6]$.

In initial tests of the reactivity of the new compounds, CaS films were deposited by ALD by using the vapor of **1** or **2** and H_2S. For both compounds, the precursor was maintained at 140 °C. At this temperature, **1** (m.p.: 110–116 °C) is a liquid, from which it evaporates at a high and consistent rate (Figure 2b). This rate of evaporation from the liquid surface is consistently reproducible, because its surface area is fixed by its container. In contrast, **2** is a solid (m.p.: 170–174 °C) at the evaporator temperature; therefore, its vaporization rate is lower and is determined by its surface area, which changes with time as the material evaporates, and thus is less reproducible.

The ALD of CaS by using the vapor of **1** with H_2S as a coreactant produced pure CaS films within the temperature range of 150–280 °C (Figure 3). The thickness of the CaS from **1** was constant over the whole length of the gas flow in the reactor (30 cm). Thus, the surface reactions of **1** were saturated over the whole substrate surface. In contrast, the films from **2** became thinner toward the end of the gas-flow path. Thus, the lower vapor pressure of **2** was not high enough to saturate its surface reactions near the end of its gas-flow path. The following discussion therefore focuses on ALD with **1**.

At temperatures below 150 °C (Figure 3a), the thickness increased owing to incomplete removal of the ligands or physical adsorption of the precursor. At temperatures over 280 °C, the thickness increased owing to decomposition of the precursor. Carbon was also detected in these higher-temperature films, which is another indication that the ALD window lies below 280 °C. Thus, the deposition operates as an ideal ALD process in the temperature range from 150 to 280 °C.

The observed ALD window covers a significantly lower and wider temperature range as compared to that with $[Ca_3(tmhd)_6]$ (325–400 °C)[11a,b] and $[Ca(tmhd)_2(tetraen)]$ (300–350 °C).[11b] This dramatic

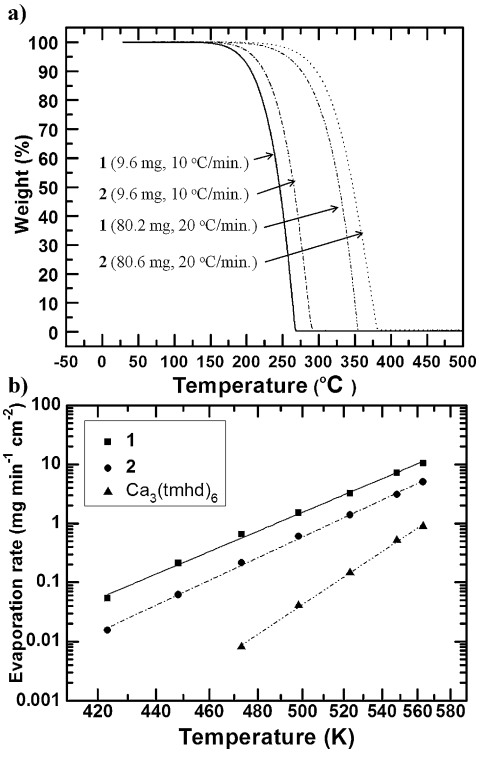

Figure 2. Thermogravimetric analysis. a) TGA curves (ramp from room temperature to 550 °C) of **1** (solid line: 9.6 mg, 10 °C min^{-1}; dash-dot-dotted line: 80.2 mg, 20 °C min^{-1}) and **2** (dash-dotted line: 9.6 mg, 10 °C min^{-1}; dotted line: 80.6 mg, 20 °C min^{-1}). b) Plot of evaporation rate (mg min^{-1} cm^{-2}, log scale) versus temperature (Kelvin, reciprocal scale) for **1** (squares, solid line), **2** (circles, dash-dotted line), and $[Ca_3(tmhd)_6]$ (triangles, dash-dot-dotted line).

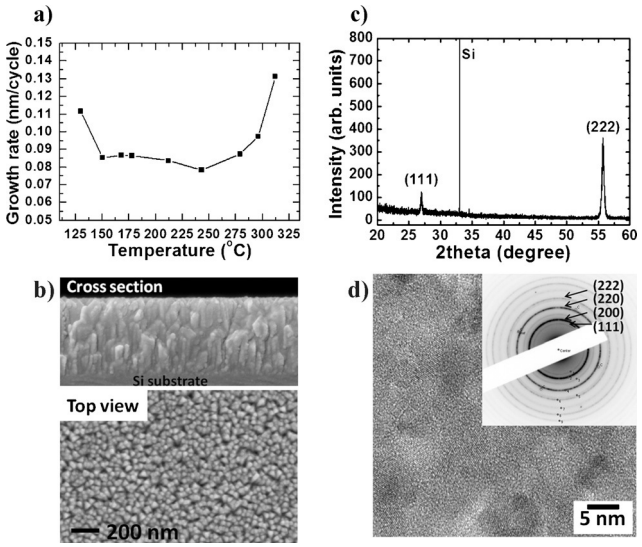

Figure 3. ALD of CaS with **1** and H_2S. a) ALD temperature window. b) SEM image (cross-section and top view) of a CaS film (540 nm, substrate temperature: 212 °C; the insulating CaS film is coated with an approximately 10 nm thick layer of sputtered gold to prevent charging) on 300 nm SiO_2 on a Si substrate. c) XRD pattern of the CaS film in (b). d) TEM image (inset: electron diffraction pattern) of a CaS film on a TEM grid substrate.

improvement to the ALD window should enrich the ALD study of alloys of CaS with other metal chalcogenides or oxides because the ALD of metal sulfides and oxides has often been performed below 300 °C.[11d] The growth rate in the ALD window (Figure 3a) was found to be 0.87 Å cycle^{-1}, which is significantly higher than that reported for [Ca_3-(tmhd)$_6$] (0.50 Å cycle^{-1}).[11a,b] In X-ray photoelectron spectroscopy (XPS) experiments for the CaS films grown in the ALD window, carbon was not detected (see Figure S6). However, in the CaS films grown at temperatures outside the ALD window (130, 296, 312 °C), carbon was detected (see Figure S6). Figure 3b shows the SEM image of a typical columnar and highly crystalline CaS film grown at 212 °C. The XRD pattern of this film (Figure 3c) shows only the (111) and (222) reflections of cubic CaS, thus indicating preferential orientation during film growth.[11d] The electron diffraction pattern of a CaS film from TEM experiments also indicates that the deposited film has the cubic (rock-salt) structure (Figure 3d; see also Figure S8).

In summary, volatile and thermally stable homoleptic, dimeric Ca^{II} amidinates were synthesized in one step through a redox reaction between calcium metal and amidines without any involvement of potential trace metal contaminants. This synthetic procedure may be applicable to Sr or Ba precursors because reactions of Sr and Br with $HN(SiMe_3)_2$ form $Sr[N(SiMe_3)_2]_2(THF)_2$ or $Ba[N(SiMe_3)_2]_2(THF)_2$ in the presence of ammonia;[19] we are currently exploring this possibility. Precursor **1** is a thermally stable liquid at its evaporation temperature, thus ensuring the rapid, stable, and reproducible delivery of vapor. The observed ALD window for CaS with **1** and H_2S is approximately twice as wide and begins 150 °C lower than the window reported for commercially available and widely employed [Ca_3(tmhd)$_6$]. Through improved volatility and lower reaction temperatures, compounds **1** and **2** provide the opportunity for increased usage of Ca in ALD, especially for the synthesis of multicomponent materials.

Acknowledgements

This research was supported in part by the Office of Naval Research (ONR) under contract number ONR N00014-10-1-0937. This study was performed in part at the Center for Nanoscale Systems (CNS) at Harvard University, a member of the National Nanotechnology Infrastructure Network (NNIN), which is supported by the National Science Foundation under NSF award no. ECS-0335765. We are grateful to Prof. T. A. Betley for letting us use his FTIR instrument.

Keywords: amidines · atomic layer deposition · calcium · redox chemistry · thin films

How to cite: *Angew. Chem. Int. Ed.* **2016**, *55*, 10228–10233
Angew. Chem. **2016**, *128*, 10384–10389

[1] M. J. Saly, F. Munnik, C. H. Winter, *J. Mater. Chem.* **2010**, *20*, 9995–10000.
[2] E. A. Paisley, M. D. Losego, S. M. Aygun, H. S. Craft, J.-P. Maria, *J. Appl. Phys.* **2008**, *104*, 114110.
[3] M. Leskelä, H. Mölsä, L. Niinistö, *Supercond. Sci. Technol.* **1993**, *6*, 627–656.
[4] O. Nilsen, E. Rauwel, H. Fjellvag, A. Kjekshus, *J. Mater. Chem.* **2007**, *17*, 1466–1475.
[5] K. Kukli, M. Ritala, T. Sajavaara, T. Hänninen, M. Leskelä, *Thin Solid Films* **2006**, *500*, 322–329.
[6] a) V. Dimitrov, S. Sakka, *J. Appl. Phys.* **1996**, *79*, 1741–1745; b) Ç. Kılıç, A. Zunger, *Appl. Phys. Lett.* **2002**, *81*, 73–75.
[7] a) B. P. Gila, M. Hlad, A. H. Onstine, R. Frazier, G. T. Thaler, A. Herrero, E. Lambers, C. R. Abernathy, S. J. Pearton, T. Anderson, S. Jang, F. Ren, N. Moser, R. C. Fitch, M. Freund, *Appl. Phys. Lett.* **2005**, *87*, 163503; b) M. D. Losego, S. Mita, R. Collazo, Z. Sitar, J.-P. Maria, *J. Vac. Sci. Technol. B* **2007**, *25*, 1029–1032.
[8] J. Vidal, S. Lany, J. Francis, R. Kokenyesi, J. Tate, *J. Appl. Phys.* **2014**, *115*, 113507.
[9] S. M. George, *Chem. Rev.* **2010**, *110*, 111–131.
[10] J. Heo, S. B. Kim, R. G. Gordon, *Appl. Phys. Lett.* **2012**, *101*, 113507.
[11] a) J. Rautanen, M. Leskelä, L. Niinistö, E. Nykänen, P. Soininen, M. Utriainen, *Appl. Surf. Sci.* **1994**, *82*, 553–558; b) T. Hänninen, I. Mutikainen, V. Saanila, M. Ritala, J. C. Hanson, M. Lskela, *Chem. Mater.* **1997**, *9*, 1234–1240; c) T. Pilvi, K. Arstila, M. Leskelä, M. Ritala, *Chem. Mater.* **2007**, *19*, 3387–3392; d) V. Miikkulainen, M. Leskelä, M. Ritala, R. L. Puurunen, *J. Appl. Phys.* **2013**, *113*, 021301; e) O. Nilsen, H. Fjellvåg, A. Kjekshus, *Thin Solid Films* **2004**, *450*, 240–247; f) M. Putkonen, T. Sajavaara, P. Rahkila, L. Xu, S. Cheng, L. Niinistö, H. J. Whitlow, *Thin Solid Films* **2009**, *517*, 5819–5824; g) J. Aarik, A. Aidla, A. Jaek, M. Leskelä, L. Niinistö, *Appl. Surf. Sci.* **1994**, *75*, 33–38.
[12] a) V. Arunasalam, S. R. Drake, M. B. Hursthouse, K. M. A. Malik, S. A. S. Miller, D. M. P. Mingos, *J. Chem. Soc. Dalton Trans.* **1996**, 2435–2442; b) I. Kazadojev, D. J. Otway, S. D. Elliott, *Chem. Vap. Deposition* **2013**, *19*, 117–124.
[13] D. J. Burkey, R. A. Williams, T. P. Hanusa, *Organometallics* **1993**, *12*, 1331–1337.

[14] W. D. Buchanan, M. A. Guino-o, K. Ruhlandt-Senge, *Inorg. Chem.* **2010**, *49*, 7144 – 7155.
[15] G. Malandrino, F. Castelli, I. L. Fragalá, *Inorg. Chim. Acta* **1994**, *224*, 203 – 207.
[16] B. Sedai, M. J. Heeg, C. H. Winter, *Organometallics* **2009**, *28*, 1032 – 1038.
[17] A. C. Dunbar, G. S. Girolami, *Inorg. Chem.* **2014**, *53*, 888 – 896.
[18] a) S. B. Kim, P. Sinsermsuksakul, A. S. Hock, R. D. Pike, R. G. Gordon, *Chem. Mater.* **2014**, *26*, 3065 – 3073; b) P. Sinsermsuksakul, J. Heo, W. Noh, A. S. Hock, R. G. Gordon, *Adv. Energy Mater.* **2011**, *1*, 1116 – 1125; c) Q. Ma, H. Guo, R. G. Gordon, F. Zaera, *Chem. Mater.* **2011**, *23*, 3325 – 3334; d) Y. Liu, M. Xu, J. Heo, P. D. Ye, R. G. Gordon, *Appl. Phys. Lett.* **2010**, *97*, 162910.
[19] S. R. Drake, D. J. Otway, *J. Chem. Soc. Chem. Commun.* **1991**, 517 – 519.
[20] a) Y. Zhang, E. K. Reeder, R. J. Keaton, L. R. Sita, *Organometallics* **2004**, *23*, 3512 – 3520; b) Z. Li, D. K. Lee, M. Coulter, L. N. J. Rodriguez, R. G. Gordon, *Dalton Trans.* **2008**, 2592 – 2597.
[21] a) M. Arrowsmith, M. R. Crimmin, M. S. Hill, S. L. Lomas, M. S. Heng, P. B. Hitchcok, G. Kociok-Köhn, *Dalton Trans.* **2014**, *43*, 14249 – 14256; b) M. Westerhausen, *Coord. Chem. Rev.* **1998**, *176*, 157 – 210; c) M. Westerhausen, *Inorg. Chem.* **1991**, *30*, 96 – 101; d) D. C. Bradley, M. B. Hursthouse, A. A. Ibrahim, K. M. A. Malick, M. Motevalli, R. Moseler, H. Powell, J. D. Runnacles, A. C. Sullivan, *Polyhedron* **1990**, *9*, 2959 – 2964.
[22] F. T. Edelmann, *Coord. Chem. Rev.* **1994**, *137*, 403 – 481.
[23] M. Westerhausen, W. Schwarz, *Z. Naturforsch. B* **1992**, 453 – 459.
[24] C. Glock, C. Loh, H. Görls, S. Krieck, M. Westerhausen, *Eur. J. Inorg. Chem.* **2013**, 3261 – 3269.
[25] a) M. L. Cole, G. B. Deacon, C. M. Forsyth, K. Konstas, P. C. Junk, *Dalton Trans.* **2006**, *3360* – 3367; b) M. L. Cole, P. C. Junk, *New J. Chem.* **2005**, *29*, 135 – 140.
[26] a) S. Harder, J. Brettar, *Angew. Chem. Int. Ed.* **2006**, *45*, 3474 – 3478; *Angew. Chem.* **2006**, *118*, 3554 – 3558; b) K. Mochida, Y. Hiraga, H. Takeuchi, H. Ogawa, *Organometallics* **1987**, *6*, 2293 – 2297.
[27] CCDC 1442724 contain the supplementary crystallographic data for this paper. These data can be obtained free of charge from The Cambridge Crystallographic Data Centre.

Received: March 8, 2016
Revised: May 22, 2016
Published online: June 28, 2016

